IoT DATA ANALYSIS FOR AVALANCHE FORECAST

SVETLANA SEGARCEANU1[1],[1] ROBERT IONUT VATASOIU[1], CARLOS JAVIER PRADOS HIJON[2], SORINA ANDREEA LOLOIU[1], GABRIEL PETRESCU[1]

Abstract. In mountainous regions worldwide, avalanches pose a significant hazard to infrastructure and human life. Avalanche identification and prediction have relied on labor-intensive and error-prone human observation and analysis. Artificial intelligence (AI) tools have become a promising means of improving the precision and speed of avalanche detection and prediction in recent years. To address this problem, we are developing an early warning system that utilizes Machine Learning techniques. This article examines the most recent research in AI techniques for avalanche detection and prediction, along with the details of our solution implementation. The system gathers and analyses data from various sensors, including meteorological and auditory sensors, to determine the potential risk of an avalanche. An analysis made on the data collected from the sensors placed in the selected region is also presented. Recent investigations have shown that AI algorithms can identify and forecast avalanches. The article discusses the potential benefits and challenges of implementing an early warning system for avalanches, highlighting the importance of continued research in this area. The research was carried out over 2 years within the MEWS project and is based on the fruitful collaboration between all partners involved in the project. The IoT stations used in the research were located in Norway. The current paper presents an analysis of the data collected in the project and a method for avalanche prediction using Feed Forward Neural Networks.

Key words: avalanches, forecasting, machine learning, Internet of Things.

1. INTRODUCTION

Densely populated mountainous regions with constant economic growth and changing climate conditions, society are increasingly exposed to natural hazards; avalanches are an important natural hazard in winter, among the deadliest natural disasters, causing damage to buildings and infrastructure, significant loss of life worldwide [1]. An eloquent example is the collapse of Marmolada in the Dolomites in July 2022, when abnormally high temperatures of around 10 °C were recorded. The collapse of a serac caused the death of 11 people and eight people were

---

[1] Beia Consult International
[2] Amplia Soluciones, Av. Europa 4, 28108, Alcobendas, Madrid, Spain

Ro. J. Techn. Sci. − Appl. Mechanics, Vol. 68, N^{os} 2–3, P. 181−196, Bucharest, 2023

DOI:10.59277/RJTS-AM.2023.2-3.06

wounded. Alpine countries such as Switzerland have experienced multiple catastrophic avalanche situations. The winter of 2017/18 was the first since the catastrophic avalanche winter in 1999 [2], during which the highest avalanche danger, level 5, was forecasted for wide areas across the Swiss Alps. In Romania in the Carpathian Mountains avalanches are also a regular phenomena. Two large avalanches took place in February 2023, in the Făgăraş Mountains, at an altitude of over 2,000 meters; one hit the Capra cottage, another was observed at Bâlea Lac, but no one was injured. The snow layer has exceeded two meters in the Bâlea Lac tourist area, where it is expected that the meteorologists have raised the degree of avalanche risk to five, a maximum degree of warning. In March 2022 two skiers, caught by an avalanche in Făgăraş, in the area of Cabana Bârcaciu, died, although 16 mountain rescuers intervened to search for them. In February 2023 an avalanche took place in the Rodna Mountains, killing a foreign tourist who was skiing.

Avalanches occur due to the failure in the snowpack. This failure is caused by stress in the snow pack, which occurs by its self-weight or other external forces. Avalanches can be classified according to the form of the starting zone (e.g. slab avalanche or punctual avalanche), form of movement (flowing avalanche, powder avalanche), or sliding surface (surface avalanche, full-depth avalanche)

There are some factors and critical conditions that can trigger an avalanche. Those factors are presented in Table 1 [3–6].

Table 1

Factors and critical conditions that trigger an avalanche

	Factor	Critical Condition
Terrain	Starting Zone	Slope greater than 28°
	Type of Surface	in relationship with snow depth
Exposure	Solar Radiation	Slope exposed to the sun
	Slope Orientation	Lee Slope
Snow condition	New snow	0-10 cm low danger 10-20 cm moderate danger 20-40 cm considerable danger 40-80 cm high danger 80-160 cm very high danger
	Snow stratification	Weak intermediate layers
	Snow depth	Smooth ground 30 cm Stony ground 60 cm
	Snow Temperature	0°C
Weather Conditions	Wind Speed	5m/s
	Relative Humidity	Wet snow
	Air Temperature	0 °C and higher OR -10 °C and lower

Another important factor would be the avalanche history of the investigated site. From the recent history point of view, the lack of an avalanche event after the last storm could be a critical factor. Information about past avalanches could be unavailable, because experts or systems do not know about it, the place is not watched by camera and nobody was there, or the camera was not functional.

Avalanche detection and prediction have historically relied on human observation and analysis of various elements, including weather patterns, snowpack conditions, and topographic features. Nevertheless, these conventional techniques take much time and can be prone to mistakes because of human variables. Artificial intelligence (AI) approaches to increase the precision and speed of avalanche detection and prediction have garnered growing interest in recent years. Machine learning algorithms can analyze large and complex datasets from various sources, including meteorological sensors, acoustic sensors, and satellite imagery, to identify the potential risk of an avalanche.

An essential step toward improving avalanche safety in mountainous places is developing an early warning system for avalanches utilizing AI techniques.

For an avalanche prediction system to work properly, it must meet several requirements related to both quality and quantity of data. These are:

- Quality of data: data should be collected during at least 8 winter seasons as weather conditions might vary very much from one winter to another.
- Quantity of data: data should be collected during enough winter seasons to provide an adequate size of the training, testing and validation sets.
- The system should be trained, tested and validated on data coming from as many as possible different winter conditions.

Large and complicated datasets may be collected and analyzed in real-time by the system, which can then deliver accurate and timely warnings to local governments and communities, thereby saving lives and minimizing avalanche damage. The AI algorithms used in the system provide a more thorough understanding of the possible risk of an avalanche, which can also see patterns and trends that may not be obvious to the human eye. The system's effectiveness in detecting and predicting avalanches has been demonstrated in recent studies. However, issues like the requirement for accurate and trustworthy data and the inherent limitations of AI algorithms need to be addressed. This article will explore the latest research in AI techniques for avalanche detection and prediction and discuss the potential benefits and challenges of implementing an early warning system for avalanches.

The present article describes the work undertaken in the framework of the Mews (Mass movement Early Warning System) project whose goal is to predict avalanches and landslides in a timely manner. The work was developed in 2021–2023. The next section presents the state of the art for avalanche detection and prediction. Section 3 presents the general features of the MEWS project and gives a description of OpenGate. Section 4 makes an analysis of the data provided in the two winter seasons during the project unfolding. Section 5 describes the early experiments aiming to predict an avalanche based on the data a day before. The system used a Feed Forward Neural Network. The last section lays the conclusions of the work.

2. MEWS PROJECT

MEWS (Mass movement Early Warning System) is a Eurostars project whose goal is to predict avalanches and landslides in a timely manner.

The goal of the project was to create a mass movement early warning system (MEWS) that can be scaled up for use in avalanche, rockfall, and landslide early detection. It gathered copious volumes of data from a variety of wireless, low-cost, field-deployed, self-powered IoT devices that house a wide variety of sensor types. A cloud-based system received the data and utilized machine learning to interpret and make decisions quickly. To illustrate the system's potential in avalanche detection, we were provided a prototype.

Similar to landslides or avalanches, mass movements provide serious dangers to people, inhabited regions, and vital transportation infrastructure. With the use of IoT technology, it is possible to create an early warning system that can accurately estimate the likelihood of an incident and lessen its effects. Lowering risk lowers costs in terms of material losses as well as community exposure.

Although mass movements are a typical occurrence in nature, they cause significant property damage and human casualties all over the world. The expenses are immeasurable, but they probably come to billions of euros annually. MEWS has the potential to significantly lower losses. We firmly believe that offering this solution to governmental bodies, small towns, and individual businesses presents a chance for income and profit.

In this regard, the project has placed 15 IoT stations in an avalanche research area in Norway, namely Ryggfonn on Strynefjellet, as it has been in operation since 1970, being one of the two large avalanche active research centers. The 15 IoT devices feature a range of sensors such as: temperature, snow depth, air temperature, air humidity, air pressure, sound, motion. The location of the devices can be seen in Fig. 1.

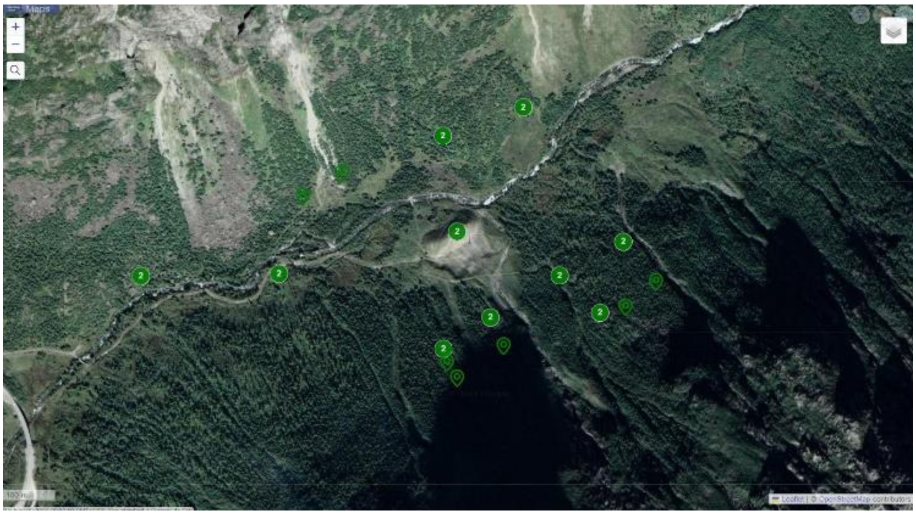

Fig. 1 – Location of IoT devices.

As previously mentioned, each of the 15 IoT stations features its own set of sensors, with which it transmits data to the main gateway. An example of an input transmitted by one of the field stations can be seen in Fig. 2.

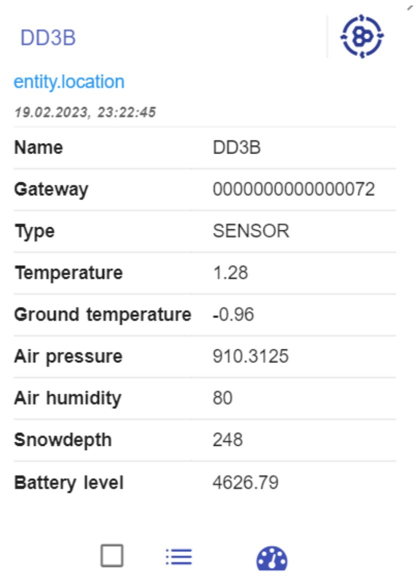
DD3B

entity.location

19.02.2023, 23:22:45

Name	DD3B
Gateway	0000000000000072
Type	SENSOR
Temperature	1.28
Ground temperature	-0.96
Air pressure	910.3125
Air humidity	80
Snowdepth	248
Battery level	4626.79

Fig. 2 – IoT Device with collected data.

Opengate. To build the detection and prediction system, all the steps for the data processing pipeline: feature engineering, feature extraction, data scaling, data encoding and dropping the unnecessary columns are hosted in the cloud. OpenGate is a cloud platform that collects the data from IoT devices, stores it, and then parses it to the prediction engine which uses AI to create predictions.

Opengate was built in the MEWS project to help the community easily use Artificial Intelligence to make predictions about incoming avalanches [14].

Opengate IoT Platform in Avalanche Prediction: Architectural Overview and Data Flow. The successful implementation of artificial intelligence in predicting snow avalanches hinges on the ability to collect, process, and interpret a wide variety of data in real time. The OpenGate IoT platform by Amplía Soluciones has been a central tool in this endeavor for the MEWS project, providing the necessary architecture for efficient data management and processing and facilitating seamless AI integration. This section outlines the platform's overall architecture for the MEWS project, its various components, and how the data flow within this system encompasses data collection, data processing, and continuous AI model training and deployment as an orchestrated interaction of various components in the OpenGate IoT platform.

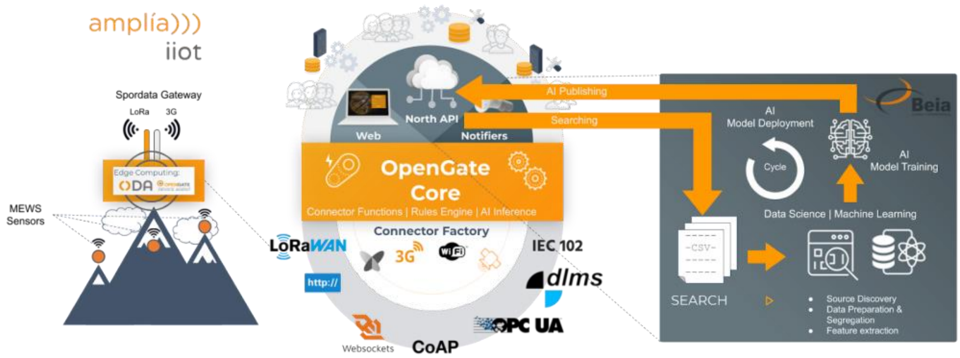

Fig. 3 – OpenGate Architecture.

The first step in this pipeline is data collection through an array of LoRa sensors spread across the Riggfonn Valley, a potential avalanche zone and the subject of the study. These sensors gather real-time environmental data that is relevant to avalanche prediction. Through LoRaWAN gateways, this data is sent to OpenGate's LoRaWAN stack. The LoRaWAN stack, created using the ChirpStack open-source LoRaWAN Network Server stack, is designed for robust and scalable data handling, ensuring efficient transmission and reception of sensor data.

Following the initial data reception through LoRaWAN, the OpenGate Connector Functions component adapts the data, aligning it to the MEWS data model requirements. This process enables the data to be seamlessly integrated with the platform's Big Data Collection Engine, which incorporates data sets and time series stores explicitly designed for the project and aligned with its data model.

The synergy of data collection, data processing, and continuous AI model refinement and deployment is critical to the system's performance. Therefore, the architecture includes two crucial components to help with the task: a powerful RESTful search engine to download the collected data for AI training purposes and an easy-to-use API to publish new AI model versions.

Once the data is collected, it moves to the Automation Rules Engine, another vital component of the OpenGate architecture. This engine is designed to continuously monitor the incoming data, checking for any new and relevant updates that could significantly contribute to avalanche prediction.

The next step is data interpretation, facilitated by OpenGate's Artificial Intelligence Inference Engine. Once the Rules Engine identifies new data, the AI Inference Engine is activated, applying the pre-trained machine learning models to analyze and predict possible avalanche risk based on the incoming data. When the AI predicts a high avalanche risk, the Rules Engine raises the alarm, triggering further preventive measures. This process exemplifies how the platform's components work in synergy, achieving an effective real-time monitoring and prediction system.

In conclusion, the OpenGate IoT platform and its comprehensive architecture are fundamental to AI-driven avalanche prediction. This solution exhibits a pioneering application of AI and IoT in environmental risk management, representing a substantial advance in snow avalanche prediction and prevention.

3. DATA STRUCTURE AND VOLUME OF DATA

In the framework of the Mews project, we were provided data collected during two seasons: winter 2021/2022 and early winter 2023. The information furnished by the deployed sensors consisted of hourly measurements of temperature, ground temperature, air pressure, air humidity, snow depth, movement, and sound. These data should usually be furnished hourly, but in reality, and inherently, some information is missing, especially in the first winter season. In the first season two sets of data were provided, in order to attune the transmission process, the second set being an improvement of the first, however data do not agree entirely. The preprocessing process included operations such as interpolation or clearing out redundant data. The missing data were interpolated linearly for a few missing hours (up to 5) from the existing data. If very few data measurements (less than 5) are present in one day, no interpolation was applied for that day, and the day was eliminated from the analysis set. Interpolation was not applied to movement and sound data, as missing movement, for example, should mean that no movement was recorded. The redundant data were averaged. Another possible processing would be normalization, a technique broadly applied on any input data in the modeling or classification phase, but we have not applied it yet.

For the two winter seasons, the avalanche research team associated a hazard risk corresponding to each day. These risks range from 1 to 4, where 1 represents the lowest risk and 4 represents the highest risk of an avalanche. More precisely, the risks were assessed during the winter seasons 2021/2022 from the 1st of December until the 22nd of March, and 2022/2023 from the 1st of December until the 2nd of February. Moreover, while the risks concern the whole region, some zones of the region are more prone than others to avalanches depending mainly on the slope and sun exposure. We have no information on the slope of each station, nor on the sun exposure (although this information might be inferred from the geographical coordinates). Figure shows the assessment of risks during the winter seasons 2021/2022, shown in green and 2022/2023, in red, in the Ryggfonn on Strynefjellet region. The image demonstrates how different the conditions in the two winter seasons are. In the first season the highest risk level was 4 and was attained in 4 days, the lowest risk was estimated for only 5 days, while in the second season the highest risk level was 3, and the lowest risk is much more frequent. Out of the 4, the transitions are from level 3 to level 4 in 3 cases, and one from level 2 to 4 (atypical). No maximum risk level, 5, was recorded. It also shows the scarcity of data: only one end of winter season (March) is included. Thus, the testing and training datasets should share this small chunk of data: if spring data were used exclusively for testing, they would not fit properly the model obtained using winter data.

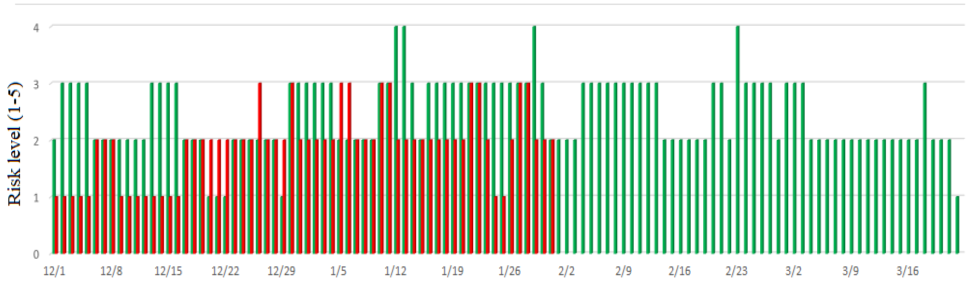

Fig. 4 – Assessment of risks during the winter seasons 2021/2022 and 2022/2023 in the Ryggfonn on Strynefjellet region.

Analysis of data – movement. We have tried to analyze the movement events in each station, and study how they relate to the assessed risk levels, and to other parameter measurements. Figs. 5–8 present the movement maps in the first season for stations DD3B9C8C0, 60209C8C0, 22879B8C01 and 3DF79B8C01, respectively. The movement data were frequent at some stations and almost missing at some others. At stations 3DF79B8C01 and 22879B8C01 there are few assessed movement events. It is also the case of stations E8339B8C01, E4B19B8C01, DF2D9C8C01, 60A39B8C01, 1CBF9B8C01. At stations DD3B9C8C0, 60209C8C0 movements happen quite often. It is also the case with station F4799B8C01. It also can be observed that there are no movement data in the first months of the winter, which might be due also to the fact that the sensors did not work properly yet. We figured the data for the month of April although we had no risk assessment for that interval, to present a more meaningful image of these events.

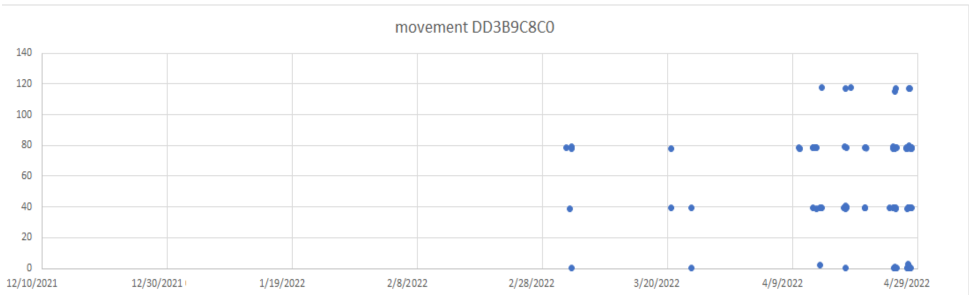

Fig. 5 – Movement map in the first winter season for station DD3B9C8C0. Measuring unit for movement: [m/s^2].

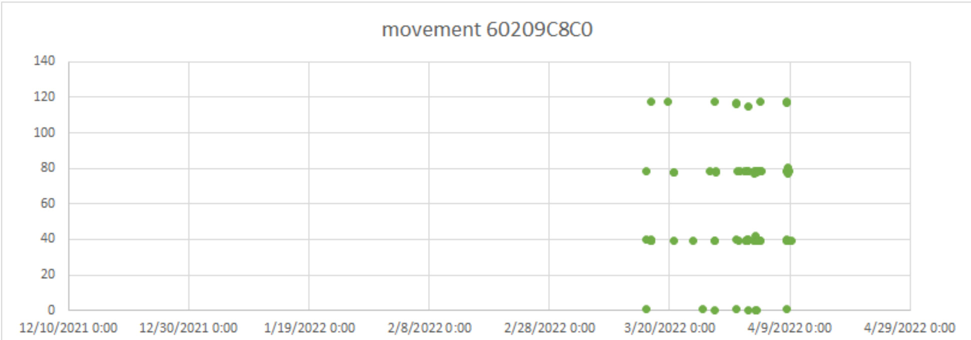

Fig. 6 – Movement map in the first season for station 60209C8C0.
Measuring unit for movement: [m/s^2].

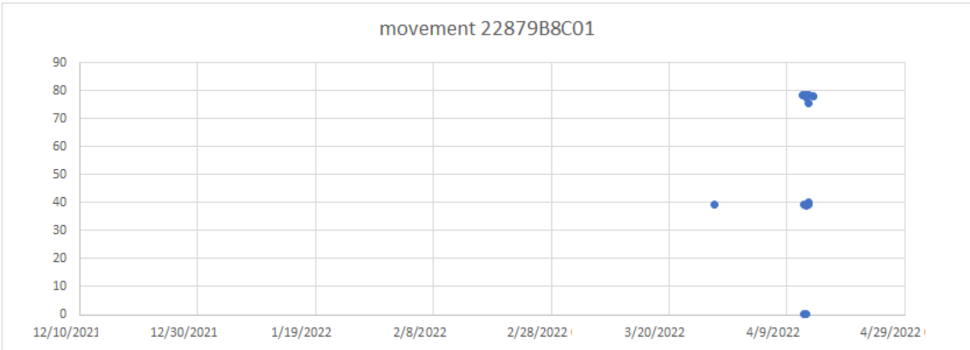

Fig. 7 – Movement map in the first winter season for station 22879B8C01.
Measuring unit for movement: [m/s^2].

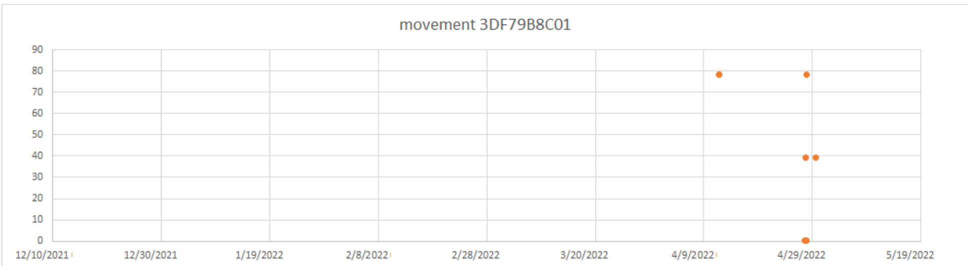

Fig. 8 – Movement map in the first season for station 3DF79B8C01.
Measuring unit for movement: [m/s^2].

Movement versus temperature. We also analyzed and compared temperature variation in several stations. For instance, Fig. 9 presents daily temperature variation at 12 pm at the station DD3B9C8C0 (with frequent movement events) versus temperature variation at 12 pm at the station 22879B8C01 (with rare movement events) in the first winter season. The temperatures seem to differ with a constant value (temperatures at DD3B9C8C0 are higher). When comparing the daily temperatures at 12 pm at stations 22879B8C01 and 3DF79B8C01, as represented in Fig. 10, we notice that they almost coincide in January and February.

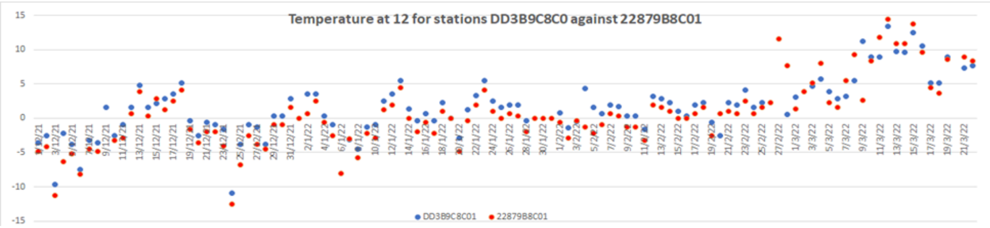

Fig. 9 – Daily variation of temperature at 12 pm for stations DD3B9C8C0 and 22879B8C01. Measuring unit for temperature: [^{0}C].

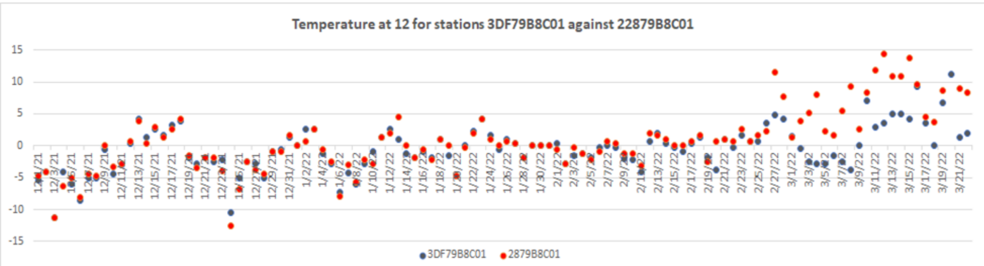

Fig. 10 – Daily variation of temperature at 12 pm for stations 3DF79B8C01 and 22879B8C01 Measuring unit for temperature: [^{0}C]

Movement versus air humidity. We made a similar analysis for air humidity. Figure 11 presents daily air humidity variation at 12 pm at the station DD3B9C8C0 (with frequent movement events) versus air humidity variation at 12 pm at the station 22879B8C01 (with few movement events) in the first winter season. The air humidity values seem to differ with a constant value (air humidity values at DD3B9C8C0 station are lower). When comparing the daily air humidity values at 12 pm in stations 22879B8C01 and 3DF79B8C01, as represented in Fig. 12, we notice that they almost coincide in January and February.

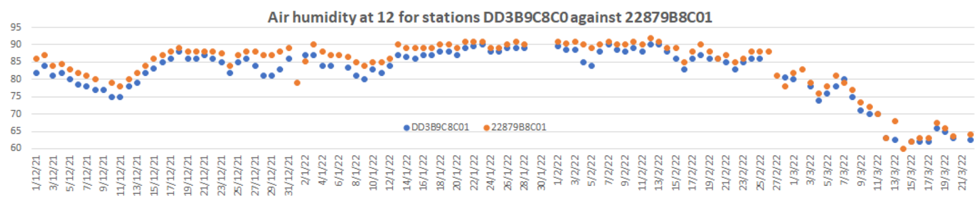

Fig. 11 – Daily variation of air relative humidity (in percents) at 12 pm for stations DD3B9C8C0 and 22879B8C01.

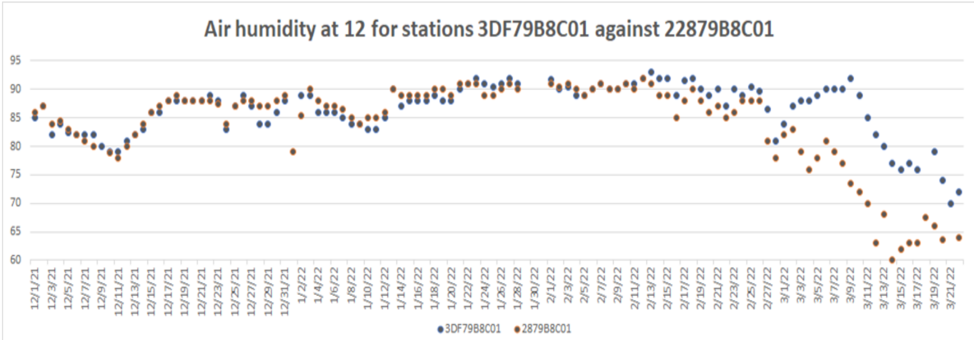

Fig. 12 – Daily variation of air relative humidity (in percents) at 12 pm for stations 3DF79B8C01 and 22879B8C01.

Air pressure versus movement. Similar experiments have shown that air pressure is not influenced by the location of the stations. Figure 13 presents daily air pressure variation at 12 pm at the station DD3B9C8C0 (with frequent movement events) versus air pressure variation at 12 pm at the station 22879B8C01 (with few movement events) in the first winter season. The values do not seem very different.

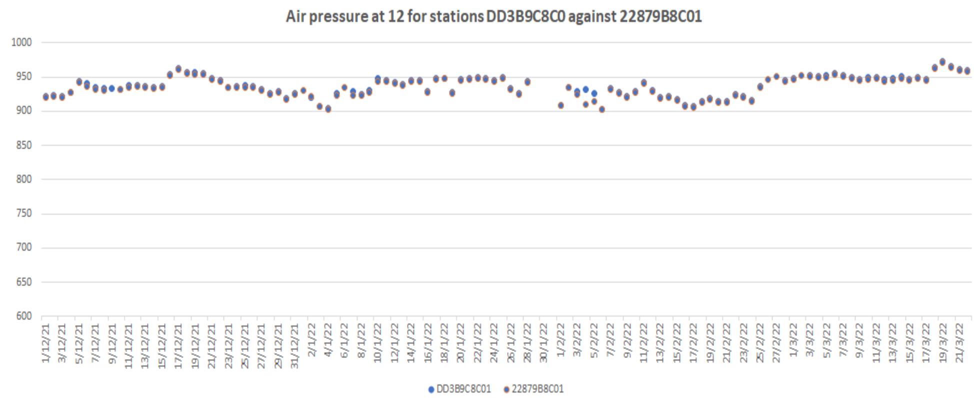

Fig. 13 – Daily variation of air pressure (in Pascals) at 12 pm for stations 3DF79B8C01 and 22879B8C01.

Snow depth. From data analysis in the first winter season, it appears that the value 256 seems to have been introduced artificially in place of missing values. In the second season there are also many missing values (some stations have no such records), replaced by 0. Figure 14 presents daily snow depth variation at 12 pm at the station DD3B9C8C0 versus snow depth variation at 12 pm at the station 22879B8C01 in the first winter season.

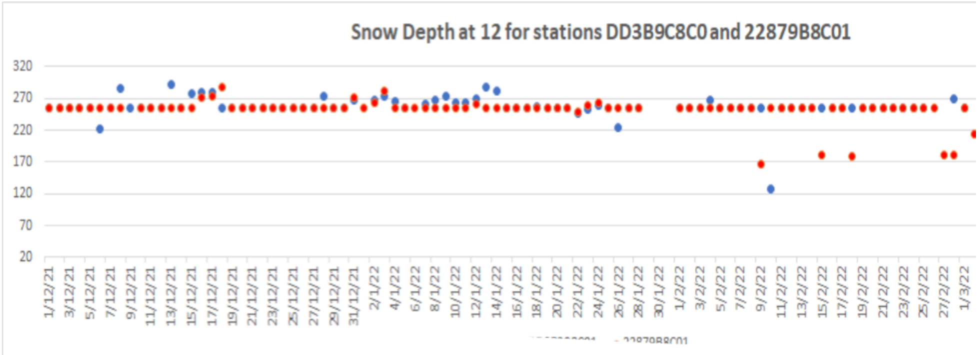

Fig. 14 – Daily variation of snow depth (measured in centimeters) at 12 pm for stations 3DF79B8C01 and 22879B8C01.

4. EARLY EXPERIMENTS USING FEED FORWARD NEURAL NETWORKS

In our first experiments we stuck to the data in the first winter season and made predictions of an avalanche risk based on the sensors data recorded the previous day (one day prediction). We used Feed Forward Neural Networks. The Neural networks architecture involved 4 layers networks. We have done experiments with 10 to 40 neurons on the first layer, 6 to 15 neurons on the second layer, 4 respectively 5 neurons on the last two layers. The Input vector was built as described subsequently. The implementation was made in MATLAB.

In the first variant we used hourly measurements of air humidity, air pressure, ground temperature, air temperature, and snow thickness, and added the risk associated with the respective day. The input vector, for a particular day in the above interval, corresponding to one of the 15 stations, looks like below where the measurements concern the previous day.

Table 2

Input vector used in the model

AH	AP	GT	S	T	AH	AP	GT	S	T	…	AH	AP	GT	S	T	R
HH:00					HH:01					…	HH:23					

AH = Air Humidity, AP = Air Pressure, GT = Ground Temperature, S = Snow Depth, T = Temperature, R = avalanche Risk

The Number of components of an input vector is 121 (5 parameters x 24 hours +1). A total of 1497 vectors were generated.

The second variant adds movement records to the input vector. In this case each daily vector contains 145 components (6 parameters x 24 hours + 1). The daily input vectors were concatenated station by station and for each station in chronological order.

This set is divided into training and test data, we chose to use 1099 vectors for training and 398 for testing. The 398 test vectors were generated randomly, thus allowing a balanced representation from all the stations (24, 28, 29, 30, 31, 22, 29, 27, 28, 13, 25, 35, 25, 31, 22, respectively for the stations "E8339B8C01", "DF2D9C8C01", "DD3B9C8C01", "DCCA9A8C01", "E4B19B8C01", "A58DA28C01", "3ECD9B8C01", "22879B8C01", "A6959B8C01", "60209C8C01", "706B9B8C01", "1CBF9B8C01", "3DF79B8C01", "F4799B8C01" , "60A39B8C01"). The distribution among the 4 risk levels was 19, 196, 168, 15, for level 1, 2, 3, 4 respectively. This approach also avoids having exclusively spring values in the testing set.

The output values were set to the risk level (1, 2, 3, 4) associated with the day when the risk was evaluated. For training, we used the risk level associated with the day before. At testing, the output of the network, when a test vector is fed, is associated with the closest value among 1, 2, 3, 4 and represents the predicted risk of avalanche for the respective day.

We have also tested the variants with reduced input vectors, corresponding to hours between 6 am to 18 am.

5. EXPERIMENTAL RESULTS

In the experiments using the measurements of Air Humidity, Air Pressure, Ground Temperature, Snow Depth, Temperature and Movement, the achieved performance was 82.41% for a network with 13, 11, 5, 4 neurons in its levels. The confusion matrix is presented in Table 3.

Table 3

Confusion matrix for the experiment using the measurements of the whole hour interval, and a network with 13, 11, 5, 4 neurons in each layer; the lines represent the assessed risk in the experiments

	Risk1	Risk 2	Risk 3	Risk 4
Assessed risk 1	68.42	1.27	0	0
Assessed risk 2	26.32	86.49	14,29	0
Assessed risk 3	5.26	12.24	81.55	20
Assessed risk 4	0	0	4.16	80

The table shows among others that risk 4 was correctly predicted in 80% of the cases (12 out of 15). The stations where risk 4 was predicted correctly for stations "DF2D9C8C01", "DD3B9C8C01", "E4B19B8C01", "3ECD9B8C01", "22879B8C01", "A6959B8C01", "1CBF9B8C01", "F4799B8C01".

There were many other similar or better performances for other Neural Network architectures, but with a lower accuracy for level 4 of risk.

In experiments with reduced data sets (excluding the measurements for hours later than 18, the results were not much different. An overall accuracy of 79.89% for a neural network with 13, 7, 5, 4 neurons on its layers and 80% correct prediction for risk level 4 of 80%, or 83.41% for a neural network with 38, 7, 5, 4 neurons on each layer, with 86.67% success in predicting level 4 (but poor performance for level 1), or 84.17% for a neural network with 37, 14, 5, 4 neurons on its layers and 73.33% prediction success for higher risk level 4. When also excluding the hour interval [0, 6] one of the best performances was 84.42, attained using a neural network with 30, 6, 5, 4 neurons, and an identification rate of 80% for risk level 4. The confusion matrix for this case is presented in Table 4.

Considering this last case, and the amount of data, the training process was accomplished in 18 iterations. Mean square error, also known as Mean square deviation, at testing was 0.1834. MATLAB also displays several progress parameters, such as Gradient (slope of tangent of graph of function) or Mu (control parameter for the back-propagation neural network). The gradient stopped value was 1.17 versus the target value 1.00-e07. Mu stopped value was 0.0001 versus 1.00+e10.

Table 4

Confusion matrix for the experiment using the measurements of the reduced hour interval, excluding the hours before 6:00 and over 18:00 achieved with a network with 30, 6, 5, 4 neurons on each of the 4 layers; the lines represent the assessed risk in the experiments, and identification rates are expressed in percent

	Risk1	Risk 2	Risk 3	Risk 4
Assessed risk 1	76.68	2.04	0	6.67
Assessed risk 2	26.32	83.16	10.71	0
Assessed risk 3	0	14.29	87.5	13.33
Assessed risk 4	0	0.51	1.79	80

6. CONCLUSIONS

The present paper has presented the framework introduced by the MEWS project for monitoring regions affected by avalanche events, with the goal of early detection of the avalanche risk. Along with MEWS, OpenGate, a new platform for facilitating AI integration used in the project, was described. We were provided data collected from IoT stations placed in Norway, for two winter seasons: 2021/2022 and early winter 2023. The information furnished by the deployed sensors consisted of hourly measurements of temperature, ground temperature, air pressure, air humidity, snow depth, movement, and sound. Although the data were quite scarce, we have tried to build a prediction system, to assess the avalanche risk based on the data from the day before, applying Feed Forward Neural Networks the input vector consisted of hourly (24 hours per day) measurements of temperature, ground temperature, air pressure, air humidity, snow depth and movement, and the assessed risk the day before. We also tried to reduce the number of hours on the day accounted for, to an interval between 6 am to 6 pm. The network had 4 layers, with a varying number of neurons on the first two layers. The accuracy achieved was about 83%. The experiments using a shorter hour interval of the day produced results comparable to those obtained for the whole interval, maybe even a little better. The method was inspired from the work [3]. They also applied Feed Forward Neural Networks on a more elaborate input vector and applied on a much more extensive set of data. The best performance achieved by their system ranges between 85% and 94%. Nevertheless, the decision is not taken automatically, but with the help of experts to interpret the output of the system.

We hope to have the chance to continue our research with a more consistent and comprehensive set of data.

Acknowledgements. This work has been supported in part by UEFISCDI Romania through the projects MEWS and SmartSense, and funded in part by European Union’s Horizon 2020 research and innovation program under grant agreement No. 883522 (S4AllCities project) and No. 872698 (HUBCAP project).

Received on November 22, 2023

REFERENCES

1. ORTNER, G., BRUNDL, M., KROPF, C. M., ROOSLI, T., BUHLER, Y., BRESCH, D. N., *Large-scale risk assessment on snow avalanche hazard in alpine regions*, Nat. Hazards Earth Syst. Sci., **23**, pp. 2089–2110, https://doi.org/10.5194/nhess-23-2089-2023, 2023.
2. WIESINGER, T., ADAMS, M., *Schnee und Lawinen in den Schweizer Alpen Winter 1998/1999*, Tech. rep., SLF, Davos, Eidg. Institut für Schnee- und Lawinenforschung SLF, https://doi.org/10.3929/ethz-b-000298085, 2007.
3. DEKANOVA, M., DUCHON, F., DEKAN, M., KYZEK, F., BISKUPIC, M., *Avalanche forecasting using neural network*, ELEKTRO, Mikulov, Czech Republic, pp. 1–5, 2018, doi: 10.1109/ELEKTRO.2018.8398359.
4. KRAJCI, P., KYZEK, F., BISKUPIC, M., SEDLAK A., *A Decade of Automatic Snow Measurements and Observations within Mountain Regions of Slovakia*, Snow an ecological phenomenon, September 2017.
5. McCLUNG, D., SCHAERER, P., *The Avalanche Handbook*, The Mountaineers Books, 2003.
6. HAEGELI, P., BAYRAKDAR, I., SCHWEIZER, J., *Application of machine learning techniques to avalanche forecasting*, Remote Sensing, **11**, *8*, p. 981, 2019.
7. VAN DER LINDEN, S. M., SCHWEIZER, J. A., STOFFEL, M., *Machine learning for avalanche forecasting: a case study in the Swiss Alps*, Natural Hazards and Earth System Sciences, **18**, *6*, pp. 1567–1581, 2018.
8. LATHAM, D. D., BAIR, E., GRANGER, G. N., *Automated snow avalanche forecasting using machine learning and acoustic sensing*, Remote Sensing, 2019.
9. BUHLER, Y., KAAB, A., HUGGEL, C., *Automated detection of snow avalanches in very high-resolution satellite images*, Remote Sensing of Environment, 2018.
10. DAS, A., MANDAL, A., KIM, K., *Avalanche hazard prediction using machine learning algorithms*, In 2019 IEEE International Conference on Electro/Information Technology (EIT), pp. 0284–0287, 2019.
11. GAO, Y., MA, W., ZHANG, H., CHEN, H., CHEN, X., *A deep learning method for forecasting snow avalanches using data from a ground-based radar,* Remote Sensing, **11**, *22*, p. 2684, 2019.

12. PAVLOVIC, N., MUGGLI, D., TECHEL, F., *A machine learning decision support system for avalanche risk management*, Natural Hazards and Earth System Sciences, **19**, *11*, pp. 2369–2385, 2019.
13. ZURBRIGGEN, N., BERNASCONI, Y., STOFFEL, L., *Avalanche risk forecasting with artificial intelligence: Development of a smartphone application for winter backcountry activities*., Journal of Outdoor Recreation and Tourism, **34**, 100346, 2021.
14. IORDACHE, G. V., SUCIU, G., SEGARCEANU, S., PETRESCU, G., VATASOIU, R. I., RODRIGUEZ, L., LANGAAS, G., *MEWS-an IoT and Cloud-Based avalanche detection and prediction platform*, 20th RoEduNet Conference: Networking in Education and Research, IEEE, 2021, pp. 1–5.